HIGH EFFICIENCY BRIDGELESS SINGLE POWER CONVERSION BATTERY CHARGER FOR ELECTRIC LOAD.

GIRIDHARAN S , GOWTHAM S,

JAYAEASWAR R , KAILASH K

M. PADMARASAN PROF. AT ELECTRICAL AND ELECTRONICS ENGINEERING

DEPT OF ELECTRICAL AND ELECTRONICS ENGINEERING

PANIMALAR INSTITUTE OF TECHNOLOGY CHENNAI

ABSTRACT

Charging batteries of light electric vehicles require chargers with high efficiency and a high-power factor. To meet this need, this paper presents a bridgeless single-power-conversion battery charger composed of an isolated step-up AC-DC converter with a series resonance circuit. The bridgeless configuration reduces the conduction losses associated with the input diode rectifier, and the series-resonance circuit reduces the reverserecovery losses of the output diodes by providing zerocurrent switching. In addition, direct and series-resonance current injection enables bidirectional core excitation by the transformer, thereby allowing high power capability. The control algorithm derived from feedback linearization is also developed, which allows the proposed charger to correct the power factor and regulate the output power in a single-stage power conversion. This simple circuit structure leads to high efficiency and a high-power factor. The theoretical concepts of the proposed charger are verified experimentally using a 1.7 kW prototype.

Index Terms— *existing system, proposed system, modes of operation, Matlab, driver circuit ,microcontroller.*

---

1 INTRODUCTION

Charging batteries of light electric vehicles require chargers with high efficiency and a high-power factor. To meet this need, this paper presents a bridgeless single-power-conversion battery charger composed of an isolated step-up AC-DC converter with a series resonance circuit. The bridgeless configuration reduces the conduction losses associated with the input diode rectifier, and the series-resonance circuit reduces the reverserecovery losses of the output diodes by providing zerocurrent switching. In addition, direct and series-resonance current injection enables bidirectional core excitation by the transformer, thereby allowing high power capability. The control algorithm derived from feedback linearization is also developed, which allows the proposed charger to correct the power factor and regulate the output power in a single-stage power conversion. This simple circuit structure leads to high efficiency and a high-power factor. The theoretical concepts of the proposed charger are verified experimentally using a 1.7 kW prototype.

2. AIM OF THE PROJECT

For the conversion of AC- DC conversion usage of electrical vehicles we attain a higher efficiency. That AC-DC conversion consist of AC- source, rectifier circuit. The rectifier circuit consist of two diodes which is responsible for AC-DC voltage conversion. There will be an inverter circuit is present. This is responsible for DC-AC conversion. That inverter circuit will consist of two switches which means MOSFET switches. For that switching device we will give pulse for that, based on the pulse the DC voltage conversion is achieved. By using the transformers, we will increase the voltage level, which means step-up transformers is used. On the transformer side again, we connect the rectifier circuits for the AC-DC voltage conversion. There will be a filter circuit is used. That filter circuit will consist of LC- filter which

is used for the pulsating output voltage into clear voltage which means DC- voltage. This is the long conversion method to get the higher DC voltage.

3. EXISTING SYSTEM

In the existing system we use the AC-DC converter for electrical vehicles with normal transformer. A rectifier is an electrical device that converts alternating current which periodically reverses direction, to direct current (DC), which flows in only one direction. The process is known as rectification, since it "straightens" the direction of current. By using the transformer, it proposed charger, which consists of an isolated bridgeless step-up AC-DC converter with a control algorithm for PFC control and to regulate the power output. The bridgeless configuration reduces conduction losses and heat-management problems related to the bridge diode. The series-resonance circuit of the secondary side provides bidirectional core excitation, which enables high power capacity and zero- current switching (ZCS), thereby reducing the reverse-recovery problem of the output diodes. In addition, because the input energy is directly distributed to the output energy without an energy buffer, efficiency is improved. To achieve a high-power factor without additional PFC circuit, we develop a control algorithm derived from feedback linearization.

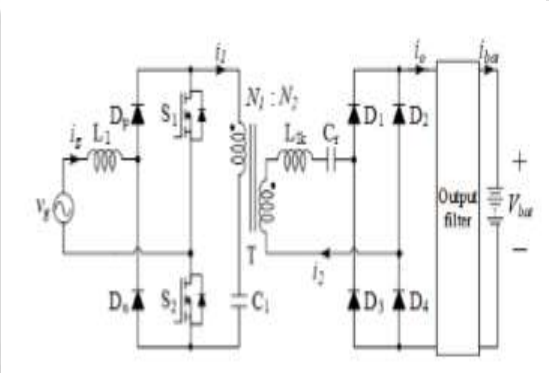

4. PROPOSED SYSTEM

In the proposed system we use the transformer-based AC-DC Converter. The proposed system of the AC-DC converter is clearly shown and the modes of operation is also clearly explained

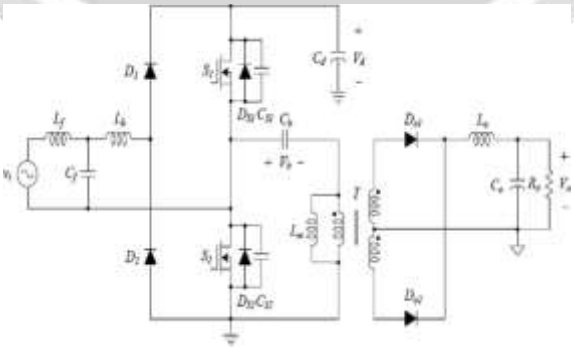

4.1. MODES OF OPERATION

In the AC-DC converter the modes of operation will be classified into two types namely. One is positive half cycle and negative half cycle. Come to the positive half cycle there will be 6 modes of operation in the AC-DC converter.

4.1.1. MODE 1(OF POSITIVE HALFCYCLE)

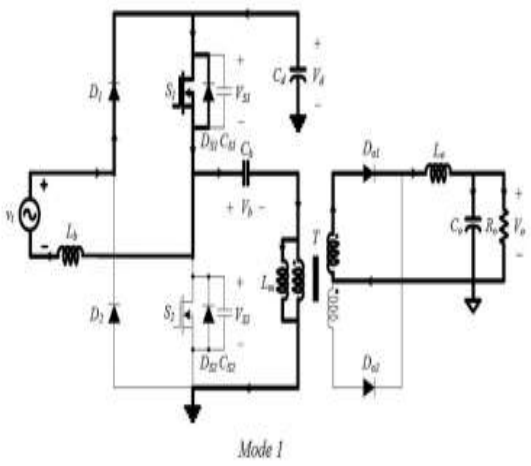

Fig. (a) shows the operation modes during Ts for a positive half line period. S1 is controlled with the duty ratio D. The conduction times of S1 and S2 are DTs and (1 − D) Ts, respectively. When S1 is turned ON, the input current ii flows through Lb, D1, and S1. When S1 is turned OFF, the input current ii flows through Lb, D1, Cd, S2, and DS 2.

4.1.2. **MODE 1(POSITIVE HALFCYCLE**

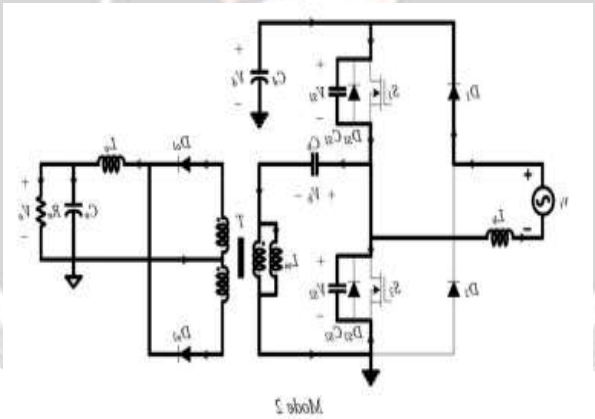

In the mode-2 positive half cycle Mode 2 [t1, t2]: At t = t1, S1 is turned OFF. The primary current ip charges CS 1 and discharges CS 2. The voltage VS 2 across S2 decreases from Vd to zero, while the voltage VS 1 across S1 increases from zero to Vd. The magnetizing current iLm and boost inductor current iLb are considered constant because the time interval during this mode is negligible compared to Ts. As long as the switch S2 is turned ON before the magnetizing current iLm changes its direction, ZVS of S2 can be assured. At the secondary side, the output filter inductor current iLo freewheels through both output diodes Do 1 and Do 2. The output diode current iDo 1 decreases while the output diode current iDo 2 increases.

5. **MATLAB**

MATLAB is a high-performance language for technical computing. It integrates computation, visualization, and programming in an easy-to-use environment where problems and solutions are expressed in familiar mathematical notation. Typical uses include

1. Math and computation

2. Algorithm development
3. Data acquisition
4. Modelling, simulation, and prototyping
5. Data analysis, exploration, and visualization
6. Scientific and engineering graphics
7. Application development, including graphical user interface building.

A common attribute of these systems is their use of power electronics and control systems to achieve their performance objectives. Sim Power Systems is a modern design tool that allows scientists and engineers to rapidly and easily build models that simulate power systems. Sim Power Systems uses the Simulink environment, allowing you to build a model using simple click and drag procedures. Not only can you draw the circuit topology rapidly, but your analysis of the circuit can include its interactions with mechanical, thermal, control, and other disciplines. This is possible because all the electrical parts of the simulation interact with the extensive Simulink modeling library. Since Simulink uses MATLAB as its computational engine, designers can also use MATLAB toolboxes and Simulink block sets. Sim Power Systems and Sim Mechanics share a special Physical Modeling block and connection line interface.

You can rapidly put Sim Power Systems to work. The libraries contain models of typical power equipment such as transformers, lines, machines, and power electronics. These models are proven ones coming from textbooks, and their validity is based on the experience of the Power Systems Testing and simulation Laboratory of Hydro-Québec, a large north.

6. DRIVER CIRCUIT

6.1 OPTO-COUPLER

We know from our tutorials about Transformer that they can not only provide a step-down voltage, but they also provide "electrical isolation" between the higher voltages on the primary side and the lower voltage on the secondary side.

In other words, transformers isolate the primary input voltage from the secondary output voltage using electromagnetic coupling by means of a magnetic flux circulating within the iron laminated core. But we can also provide electrical isolation between an input source and an output load using just light by using a very common and valuable electronic component called an **Optocoupler**.

In other words, transformers isolate the primary input voltage from the secondary output voltage using electromagnetic coupling by means of a magnetic flux circulating within the iron laminated core. But we can also provide electrical isolation between an input source and an output load using just light by using a very common and valuable electronic component called an **Optocoupler**.

Optocoupler are available in four general types, each one having an infra-red LED source but with different photo-sensitive devices. The four optocoupler are called the *Photo-transistor, Photo-Darlington, Photo-SCR and Photo-Triac***.**

In other words, transformers isolate the primary input voltage from the secondary output voltage using electromagnetic coupling by means of a magnetic flux circulating within the iron laminated core. But we can also provide electrical isolation between an input source and an output load using just light by using a very common and valuable electronic component called an **Optocoupler**.

Optocoupler are available in four general types, each one having an infra-red LED source but with different photo-sensitive devices. The four optocoupler are called the *Photo-transistor, Photo-Darlington, Photo-SCR and Photo-Triac*

In this application, the optocoupler is used to detect the operation of the switch or another type of digital input signal. This is useful if the switch or signal being detected is within an electrically noisy environment. The output can be used to operate an external circuit, light or as an input to a PC or microprocessor.

6.2. AN OPTO TRANSISTOR DC SWITCH

As well as detecting DC signals and data, Opto-Triac isolators are also available which allow AC powered equipment and mains lamps to be controlled. Opto-coupled triacs such as the MOC 3020, have voltage ratings of about 400 volts making them ideal for direct mains connection and a maximum current of about 100mA. For higher powered loads, the opto-Triac may be used to provide the gate.

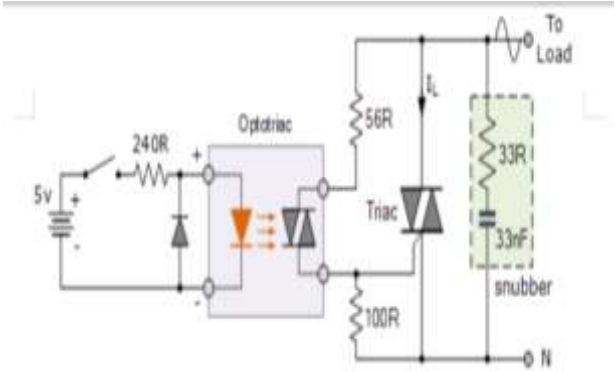

7.MICROCONTROLLER

7.1 PIN DIAGRAM

This document contains device specific information for the dsPIC30F4011/4012 device. The dsPIC30F devices contain extensive Digital Signal Processor (DSP) functionality within a high performance 16bit microcontroller (MCU) architecture block diagrams for the dsPIC30F4011 and dsPIC30F4012 de vice.

7.2. DATA STORED

- The upper 32 Kbytes of data space memory can be mapped into the lower half (user space) of program space at any 16K program word boundary, defined by the 8-bit Program Space Visibility Page (PSVPAG) register.
- This lets any instruction access program space as if it were data space, with a limitation that the access requires an additional cycle.
- Moreover, only the lower 16 bits of each instruction word can be accessed using this method.

The program address space is 4M instruction words. It is addressable by the 23-bit PC, table instruction Effective Address (EA), or data space EA, when program space is mapped into data space, as defined by Table 3-1. Note that the program space address is incremented by two between successive program words, in order to provide compatibility with data space addressing.

User program space access is restricted to the lower 4M instruction word address range (0x000000 to 0x7FFFFE), for all accesses other than TBLRD/TBLWT, which use TBLPAG to determine user or configuration space access. In Read/Write instructions bit 23 allows access to the Device ID, the User ID and the configuration bits. Otherwise, the bit 23 is always clear. The upper 32 Kbytes of data space may optionally be mapped into any 16K word program space page. This provides transparent access of stored constant data from X data space, without the need to use special instructions (i.e., TBLRDL/H, TBLWTL/H instructions).

Program space access through the data space occurs if the MS bit of the data space EA is set and program space visibility is enabled, by setting the PSV bit in the Core Control register (CORCON). The functions of CORCON are discussed in Section 2 DSP Engine. Data accesses to this area add an additional cycle to the instruction being executed, since two program memory fetches are required. Note that the upper half of addressable data space is always part of the X data space. Therefore, when a DSP operation uses program space mapping to access this memory region, Y data space should typically contain state (variable) data for DSP operations, whereas X data space should typically contain coefficient (constant) data. Although each data space address, 0x8000 and higher, maps directly into a corresponding program memory address.

8. CONCLUSION

This paper proposes a high-efficiency bridgeless battery charger for light EVs and analyze its performance both theoretically and experimentally. Eliminating the input bridge diode reduces the conduction losses, and the use of a series resonance circuit provides ZCS and alleviates the reverse recovery problem for output diodes. Bidirectional core excitation of the transformer leads to a higher power capability than conventional bridgeless converters. Since the proposed charger applies the electrolytic capacitorless scheme with a sinusoidal-like dc current on the batter side, the input ac power is directly transferred to the battery side and the efficiency is improved. In addition, the proposed control algorithm enables the charger to correct the power factor and regulate the output through single-power-conversion. With these advantages, the proposed charger offers high efficiency and high-power quality. The maximum efficiency of 96.2% is achieved from the simple circuit structure and the soft-switching features for the output diodes. Also, the use of the control algorithm gives a power factor of near unity for a universal grid voltage. Therefore, the proposed charger with its control algorithm is an effective solution for EVs, which require high charging efficiency, power factor, and a simple structure.

REFRENCE

REFERENCE

[1] S. Haghbin, S. Lundmark, M. Alakula, and O. Carlson, “Grid-connected integrated battery chargers in vehicle applications: Review and new solution,” IEEE Transactions on Industrial Electronics, vol. 60, no. 2, pp. 459–473, 2013.

[2] M. Yilmaz and P. T. Krein, “Review of battery charger topologies, charging power levels, and infrastructure for plug-in electric and hybrid vehicles,” IEEE Transactions on Power Electronics, vol. 28, no. 5, pp. 2151–2169, 2013.

[3] A. Khaligh and S. Dusmez, “Comprehensive topological analysis of conductive and inductive charging solutions for plug-in electric vehicles,” IEEE Transactions on Vehicular Technology, vol. 61, no. 8, pp. 3475– 3489, 2012.

[4] S.-G. Jeong, W.-J. Cha, S.-H. Lee, J.-M. Kwon, and B.-H. Kwon, “Electrolytic Capacitor-Less Single-Power-Conversion On-Board Charger With High Efficiency,” IEEE Transactions on Industrial Electronics, vol. 63, no. 12, pp. 7488–7497, 2016.

[5] B. Whitaker, A. Barkley, Z. Cole, B. Passmore, D. Martin, T. R. McNutt, A. B. Lostetter, J. S. Lee, and K. Shiozaki, “A high-density, highefficiency, isolated on-board vehicle battery charger utilizing silicon carbide power devices,” IEEE Transactions on Power Electronics, vol. 29, no. 5, pp. 2606–2617, 2014.

[6] D. S. Gautam, F. Musavi, M. Edington, W. Eberle, and W. G. Dunford, “An automotive onboard 3.3-kW battery charger for PHEV application,” IEEE Transactions on Vehicular Technology, vol. 61, no. 8, pp. 3466– 3474, 2012.

[7] S. Kim and F.-S. Kang, "Multifunctional onboard battery charger for plug-in electric vehicles," IEEE Transactions on Industrial Electronics, vol. 62, no. 6, pp. 3460–3472, 2015.

[8] K. Yao, Y. Wang, J. Guo, and K. Chen, "Critical Conduction Mode Boost PFC Converter with Fixed Switching Frequency Control," IEEE Transactions on Power Electronics, 2017.

[9] T. Mishima, K. Akamatsu, and M. Nakaoka, "A high frequency-link secondary-side phase-shifted full-range soft-switching PWM DC-DC converter with ZCS active rectifier for EV battery chargers," IEEE Transactions on Power Electronics, vol. 28, no. 12, pp. 5758–5773, 2013.

[10] M. Kwon and S. Choi, "An Electrolytic Capacitorless Bidirectional EV Charger for V2G and V2H Applications," IEEE Transactions on Power Electronics, vol. 32, no. 9, pp. 6792–6799, 2017.

[11] K.-M. Yoo, K.-D. Kim, and J.-Y. Lee, "Single-and three-phase PHEV onboard battery charger using small link capacitor," IEEE Transactions on Industrial Electronics, vol. 60, no. 8, pp. 3136–3144, 2013.

[12] L. Wang, B. Zhang, and D. Qiu, "A Novel Valley-Fill Single-Stage Boost-Forward Converter With Optimized Performance in UniversalLine Range for Dimmable LED Lighting," IEEE Transactions on Industrial Electronics, vol. 64, no. 4, pp. 2770–2778, 2017.

[13] Y. Wang, N. Qi, Y. Guan, C. Cecati, and D. Xu, "A single-stage LED driver based on SEPIC and LLC circuits," IEEE Transactions on Industrial Electronics, vol. 64, no. 7, pp. 5766–5776, 2017.

[14] G. Moschopoulos and P. Jain, "Single-phase single-stage power-factorcorrected converter topologies," IEEE Transactions on Industrial Electronics, vol. 52, no. 1, pp. 23–35, 2005.

[15] S. Li, J. Deng, and C. C. Mi, "Single-stage resonant battery charger with inherent power factor correction for electric vehicles," IEEE Transactions on Vehicular Technology, vol. 62, no. 9, pp. 4336–4344, 2013.